Effect of oxygen atmosphere on the structure and refractive index dispersive behavior of $KTa_{0.5}Nb_{0.5}O_3$ thin films prepared by PLD on Si(0 0 1) substrates

Wenlong Yang, Zhongxiang Zhou *, Bin Yang, Yongyuan Jiang, Yanbo Pei, Hongguo Sun, Ying Wang

Department of Physics, Harbin Institute of Technology, Harbin 150001, PR China

ABSTRACT

$KTa_{0.5}Nb_{0.5}O_3$ thin films were deposited on Si(0 0 1) substrates by pulsed laser deposition (PLD) with different oxygen pressures (10 Pa, 15 Pa, 20 Pa, 25 Pa and 30 Pa). The effect of oxygen atmosphere on the structure and refractive indices of the films were studied. It is found that the phase structure, the scale of the grains, the surface roughness and the optical properties of the films are sensitive to oxygen atmosphere variation. The refractive indices of the films were investigated by ellipsometer and the dispersive behavior was analyzed by Cauchy dispersion model. The films grown with 15 Pa oxygen pressure show the pure perovskite structure and the dispersion behaviors possess the normal dispersion shape; and other influence on the quality and properties of $KTa_{0.5}Nb_{0.5}O_3$/Si(0 0 1) films were discussed.

© 2011 Elsevier B.V. All rights reserved.

1. Introduction

As the exploding development of electronic devices, strong requirements of miniaturization and integration motivate the progress of functional films. Ferroelectric film has attracted much attention due to its potential applications on nonvolatile memories, pyroelectric detectors, microwave devices, electro-optic switches and modulators [1–5]. Recently, many researches have focused on functional ferroelectric films such as lead zirconate titanate (PZT), barium strontium titanate (BST), barium sodium niobate (BNN), and so on [6–9]. Among ferroelectrics, another family of materials, $KTa_{1-x}Nb_xO_3$ (KTN) is well known for its excellent dielectric permittivity and low loss tangent [1,10]. Compared with other compounds, the phase structures and the properties of KTN can be modulated by different Ta/Nb ratio [11,12]. Therefore, suitable composition of KTN can be selected for different applications. For example, outstanding optical properties and large electro-optic effect could be obtained when the Ta/Nb ratio is bigger than or equal to 0.65/0.35 [13]; and excellent ferroelectric properties could be obtained when the Ta/Nb ratio is smaller than 0.65/0.35 [2,14].

Bulk KTN single crystals synthesized from high temperature melts were limited in device application due to the occurrence of lamellar growth, twins, etc. [15]. Correspondingly, KTN thin films are more convenient for electronic and optical devices application,

because films can afford the possibility of integration with very-large-scale silicon integration technologies [16,17]. Recently, KTN films have been obtained by various physical and chemical methods [2,14,18–24]. Among those processes, pulsed laser deposition (PLD) is the most superior [1,17,20,21]. The growth temperature is about 50–100 °C lower than other technologies, because target ablated by laser can create a highly energetic plasma, leading to nonequilibrium growth condition. Thus, high-quality films can be obtained at a fairly low substrate temperature [25]. Due to the convenience of targets change, the potassium loss could be compensated by using the K-enriched ceramic targets or segmented targets [1,2,17]. Meanwhile, the orientation and microstructure of the films can be controlled by the growth condition, such as substrate temperature, oxygen atmosphere and substrate-target distance.

In this paper, $KTa_{0.5}Nb_{0.5}O_3$ thin films with different growth oxygen atmospheres were prepared on Si(0 0 1) substrates by PLD technique. The effect of the oxygen atmosphere on the structure, microtopography and the refractive indices of the films were investigated. The refractive index dispersion behavior was analyzed by Cauchy model.

2. Experimental procedure

The K-enriched KTN ceramics were used for the targets and $KTa_{0.5}Nb_{0.5}O_3$ (KTN50) thin films were deposited on Si(0 0 1) substrates. The details of the target preparation and deposition experiment could be found in previous papers [26,27]. A KrF excimer laser (LPX205i, Lambda Physik, 248 nm), with repetition

* Corresponding author. Tel.: +86 451 86414130; fax: +86 451 86414141.
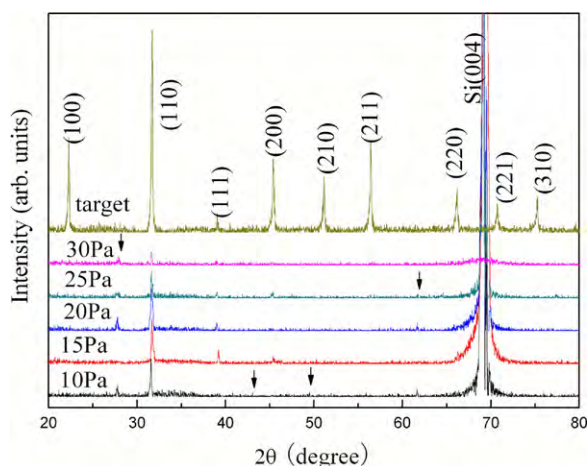*E-mail address:* zhouzx@hit.edu.cn (Z. Zhou).

Fig. 1. XRD patterns of K enriched KTN ceramic targets and KTN50 films on Si(0 0 1) substrates grown with different oxygen pressure (10 Pa, 15 Pa, 20 Pa, 25 Pa and 30 Pa).

rate of 5 Hz and pulse energy fluence 2.0 J/cm^2, was focused on a rotating target set in the chamber through a quartz window for thin films growth with 30 min. The growth temperature of the substrate was 700 °C, target-substrate distance was set at 6 cm, and the oxygen atmosphere ranged from 15 Pa to 30 Pa. After deposition, the thin films were natural cooling to room temperature in the chamber with the same oxygen pressure. The crystalline structures of the films were investigated by XRD (XRD-6000, Shimadzu, Japan). The morphology and the surface roughness were evaluated by SEM (S-4700, Hitachi, Japan) and SPM (CSPM500, Ben Yuan Ltd., China). The refractive index properties were measured by ellipsometer.

3. Results and discussion

The XRD patterns of the K-enriched KTN ceramic targets and KTN50/Si(0 0 1) films prepared with different oxygen pressures (10 Pa, 15 Pa, 20 Pa, 25 Pa and 30 Pa) are shown in Fig. 1. The ceramic targets were found to be tetragonal symmetry with the perovskite type ABO$_3$ subcell. The diffraction peaks of KTN50 films reveal a mixture of pyrochlore (shown as arrow in Fig. 1) and perovskite phases. The experimental results have also shown that growth atmosphere influences the structure of the films strongly. As is shown in Fig. 1, the intensities of (1 1 0), (1 1 1) reflection peaks and the content of the pyrochlore phase are sensitive to the variation of the oxygen pressure. The intensities of the (1 0 0) reflections with 15 Pa and 20 Pa growth atmospheres are obviously bigger than that of 10 Pa. And then, the intensity becomes weaker with the increase of the oxygen pressure. Different from the (1 0 0) reflection, the intensity of (1 1 1) reflection decreases directly with the increase of the oxygen pressure. It is important to indicate that the pyrochlore phase would disappear when the growth oxygen pressure is 15 Pa and the films of pure perovskite phases are obtained, which indicates the optimal growth oxygen atmosphere. It is known that the defect-potassium niobate pyrochlore phase would appear in the lower oxygen pressure caused by the high volatility of alkaline [1,2,14]. Also the oxygen pressure cannot be set too high, because higher oxygen pressure indicates intensive collision between the particles of the plasma and oxygen molecules. The scattering of potassium may play important role in the second phase formation with higher oxygen pressure [28].

Fig. 2 exhibits the SEM micrographs taken from the surface and cross section of the KTN50 films on Si(0 0 1) substrates grown with different oxygen pressures. It can be seen from Fig. 2(a)–(e) that all the films reveal crack-free microstructure with uniform grains.

The size of the grains increases with the increasing oxygen pressure. In Fig. 2(a) and (b), the sizes of the grains are smaller when the grown oxygen pressure is lower (10 Pa and 15 Pa). The size of the grains becomes more than 100 nm when the oxygen pressure is or exceeds 20 Pa, as is seen in Fig. 2(c)–(e). This phenomenon indicates that high oxygen pressure is helpful to grains growth. From the images, we can find the surface of the films very smooth when the growth oxygen pressure ranges from 10 Pa to 15 Pa. Then, the surface roughness gets worse and the defects increase as the grains grow with higher oxygen pressures. It can be seen from the cross section of the films with different oxygen pressures that the interfaces between the films and Si(0 0 1) substrates are very clear, as shown in Fig. 2(f)–(h). The thickness of the films is around 100 nm. The undulation of the surface roughness has close relationship with the growth atmosphere. The surfaces of KTN50 films grown with lower oxygen pressure are smoother than those grown with higher oxygen pressure, which corresponds with the results of the surface images.

In order to study the microstructure and the surface topography of the KTN50 films further, the SPM surface images of the films deposited on Si(0 0 1) substrates with different oxygen pressures are taken, as shown in Fig. 3. The results indicate that surface roughness of the KTN50 films is quite sensitive to the variation of growth atmosphere. The surface roughness average (RA) and root mean square (RMS) increase from 8.2 nm and 10.6 nm for 10 Pa to 27.2 nm and 34.5 nm for 30 Pa, which are calculated from random areas about 12 μm × 12 μm of the films. It is obvious that the surface roughness gets worse with the increasing oxygen pressure. This kind of variation confirms the results from the surface and cross section SEM micrographs of the films. The surface morphology is considered to be correlated with the diffusion coefficient of the adsorption particles, which is strongly influenced by oxygen pressure [28,29]. When the oxygen pressure is lower, the collision between the particles of the plasma and oxygen molecules is weaker and the higher kinetic energy particles would arrive at the substrates, which result in the larger diffusion coefficient of the deposition particles and the smoother surface morphology. Conversely, the diffusion coefficient of deposition particles is smaller and the surface roughness of the films gets worse, when the oxygen pressure becomes higher.

The refractive index of the KTN50/Si(0 0 1) films with wavelength ranging from 380 nm to 900 nm were measured by ellipsometer with light incident angle about 70°, as shown in Fig. 4. During the analysis, the birefringence of the KTN50 films are not taken into account, because the lattice parameters of the films are very similar with those of the cubic phase and the orientation of the films may decrease that effect [30]. The calculated thickness of the KTN50 films with different oxygen pressures range from 90 nm to 120 nm, which are consistent with SEM observations for cross-sections of the thin films. And all the films possess significant wavelength dependent dispersion behaviors, which could be described by Cauchy mode dispersion formula

$$n = A + \frac{B}{\lambda^2} + \frac{C}{\lambda^4} \quad (\lambda \text{ in micron})$$

where A, B and C are dispersive parameters, and the values are calculated by experimental curve fitting, as shown in Table 1.

It can be seen from Fig. 4 that the refractive index dispersion behaviors of KTN films grown with 10 Pa and 15 Pa oxygen pressures show the typical shape of the normal dispersion curve, the refractive indices n decrease with increasing the wavelength from 380 nm to 900 nm. The dispersion curves are quite different for the films grown with 20 Pa, 25 Pa and 30 Pa oxygen pressures, which present abnormal dispersion shape, and broad peaks around 450 nm wavelength. The refractive indices n firstly increase with wavelength until 450 nm, and then decrease. This might be
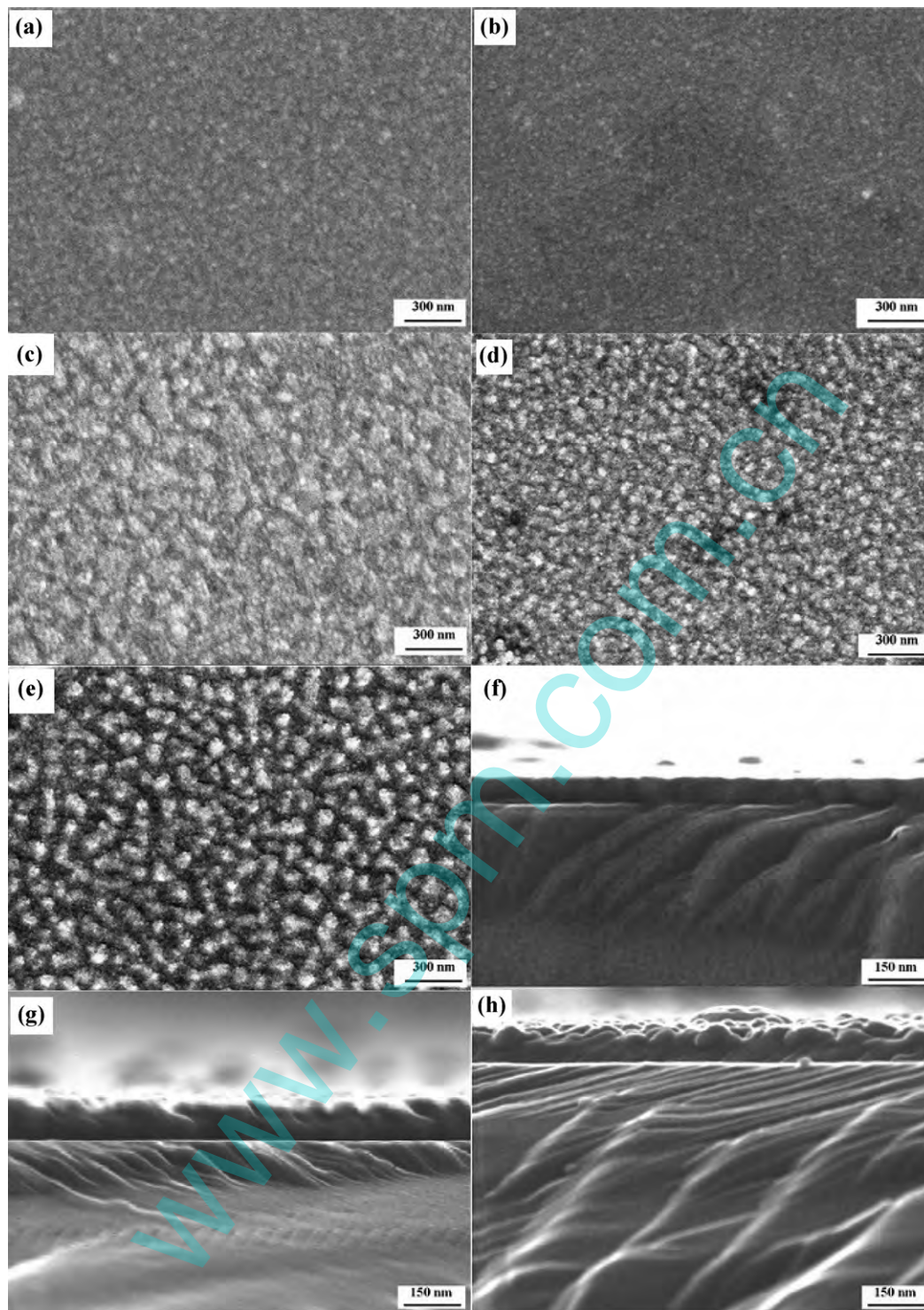
Fig. 2. Microstructures of KTN50 films grown on Si(0 0 1) substrates with different oxygen pressures, (a) and (f) 10 Pa, (b) 15 Pa, (c) and (g) 20 Pa, (d) 25 Pa, (e) and (h) 30 Pa.

explained by the increased defects such as potassium deficiency pyrochlore phase and microspore. The general values of refractive indices increase when the oxygen pressure increases from 10 Pa to 15 Pa, and then decrease for even higher oxygen pressure. In other words, the films grown with 15 Pa oxygen pressure (pure perovskite phase) possess the biggest value of the refractive index in the given wavelength compared with those grown with other oxygen pressures. The refractive indices of the films with 20 Pa approach to those of 15 Pa, and much bigger than those of other oxygen pressures.

The dispersive behavior of KTN50 thin films grown with 15 Pa on Si(0 0 1) substrates and that of KTN crystal are similar [11,20,26,31]. The comparability indicates the good crystalline quality of our films. It is worth mentioning that the refractive indices of the films grown with 15 Pa oxygen pressure is a little smaller than that of bulk materials and films grown on the small lattice mismatch substrates in given wavelength [11,20,26,31]. This disaccord is considered to be correlated with the bigger lattice mismatch (more than 20%) between the KTN50 films and Si(0 0 1) substrate. The lattice parameters a and c of the KTN50 films were calculated, to be 3.993 and
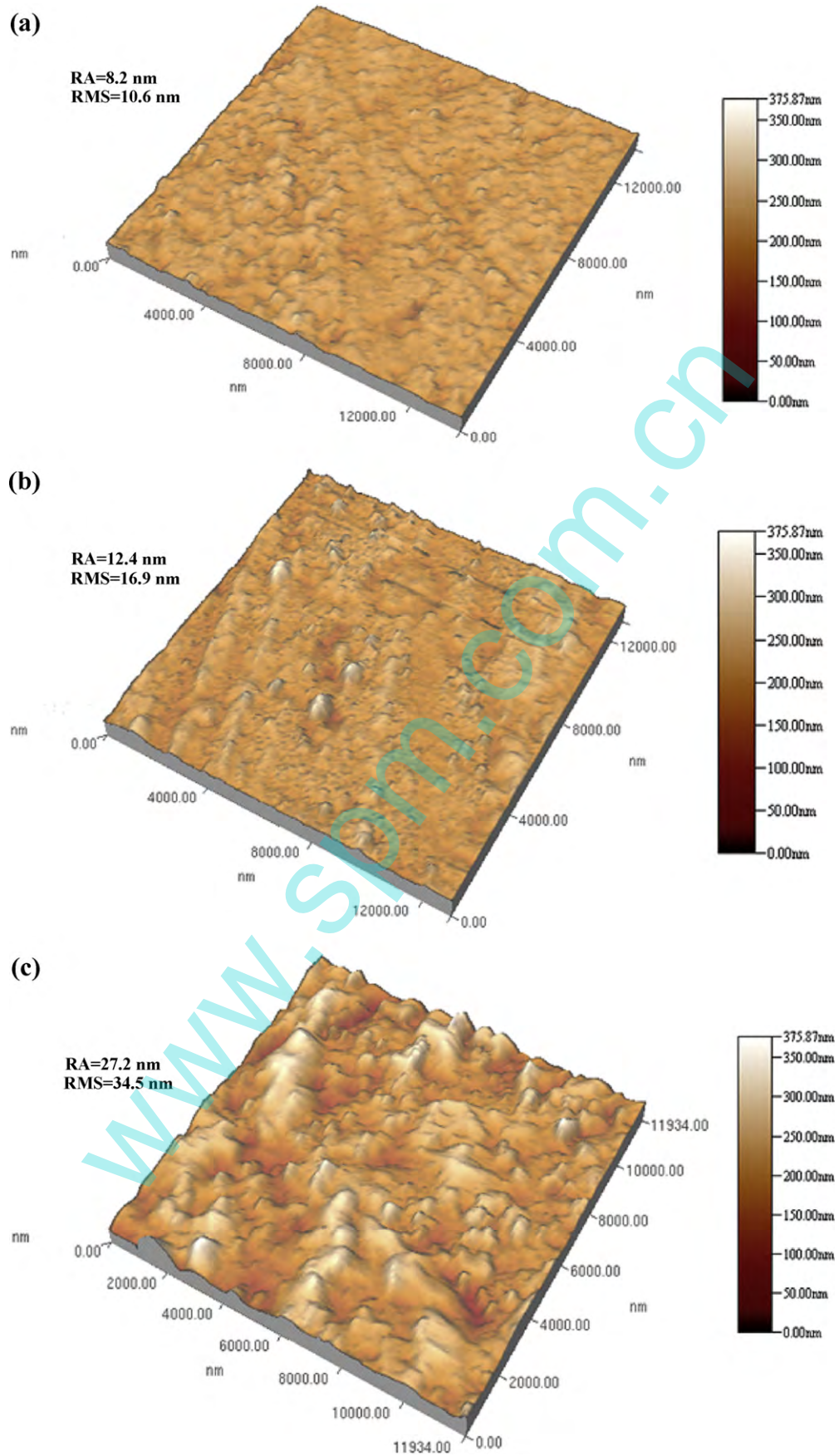
Fig. 3. Surface topographies of KTN50 films grown on Si(0 0 1) substrates with different oxygen pressures, (a) 10 Pa, (b) 20 Pa and (c) 30 Pa.

Table 1
Cauchy dispersive parameters of KTN50 films grown on Si(0 0 1) substrates with different oxygen pressures.

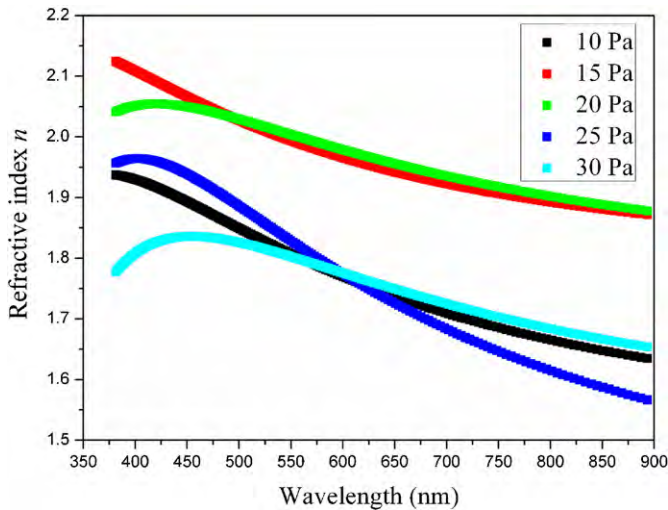| Oxygen pressure	A	B	C
10 Pa	15.2 ± 0.01	0.109 ± 0.002	−0.0071 ± 0.0002
15 Pa	1.80 ± 0.02	0.078 ± 0.003	−0.0037 ± 0.0004
20 Pa	1.75 ± 0.02	0.120 ± 0.007	−0.0110 ± 0.0005
25 Pa	1.26 ± 0.01	0.202 ± 0.004	−0.0168 ± 0.0004
30 Pa	1.50 ± 0.05	0.15 ± 0.03	−0.016 ± 0.003

Fig. 4. Refractive index dispersion behavior of KTN50 films grown with different oxygen pressures.

4.020 Å, and parameter of Si(0 0 1) substrate is 5.430 Å [26]. The parameters of MgO (1 0 0) and Pt are 4.212 Å and 3.924 Å respectively; thus the mismatches with KTN50 films are smaller than 6%. As is known to all, mismatch is also closely related to the structure and the defects of the films [1,18–21].

4. Conclusion

Crack-free $KTa_{0.5}Nb_{0.5}O_3$ thin films were successfully deposited on Si(0 0 1) substrates by pulsed laser deposition with different oxygen atmospheres (10 Pa, 15 Pa, 20 Pa, 25 Pa and 30 Pa). The crystalline structures were analyzed by X-ray diffraction, and the microtopographies with different growth atmosphere were investigated by SEM and SPM. It is found that the phase structure, the scale of the grains, the surface roughness and the optical properties of the films are closely related to oxygen atmosphere. The grains of the films increase with the increasing oxygen pressure, and the surface roughness gets worse as well. The refractive indices of the films were investigated by ellipsometer. The dispersive behavior was analyzed by Cauchy dispersion model. The films grown with 15 Pa oxygen pressure show the pure perovskite structure and the dispersion behaviors possess the normal dispersion shape, the dispersive parameters A, B and C are 1.80 ± 0.02, 0.078 ± 0.003 and −0.0037 ± 0.0004, respectively.

References

[1] W. Peng, M. Guilloux-Viry, S. Deputier, V. Bouquet, Q. Simon, A. Perrin, A. Dauscher, S. Weber, Appl. Surf. Sci. 254 (2007) 1298.
[2] A. Nazeri, Appl. Phys. Lett. 65 (1994) 295.
[3] P.B. Ishai, C.E.M. de Oliveira, Y. Ryabov, Y. Feldman, A.J. Agranat, Phys. Rev. B 70 (2004) 132104.
[4] C. Kang, J.H. Park, D. Shen, H. Ahn, M. Park, D.J. Kim, J. Sol-Gel Technol. 58 (2011) 85.
[5] H.Y. Zhang, X.H. He, Y.H. Shih, K.S. Harshavardhan, L.A. Knauss, Opt. Lett. 22 (1997) 1745.
[6] Y.B. Jeon, R. Sood, J.-H. Jeong, S.-G. Kim, Sens. Actuator A-Phys. 122 (2005) 16.
[7] H. Simons, J. Daniels, W. Jo, R. Dittmer, A. Studer, M. Avdeev, J. Rödel, M. Hoffman, Appl. Phys. Lett. 98 (2011) 082901.
[8] T.H. Fang, W.J. Chang, C.M. Lin, L.W. Ji, Y.S. Chang, Y.J. Hsiao, Mater. Sci. Eng. A-Struct. 426 (2006) 157.
[9] O. Hirotaka, K. Akinori, N. Yoshifumi, J. Alloys Compd. 473 (2009) 567.
[10] W. Peng, V. Bouquet, S. Deputier, Q. Simon, M. Guilloux-Viry, A. Perrin, Integr. Ferroelectr. 93 (2007) 126.
[11] F.S. Chen, J.E. Geusic, S.K. Kurtz, J.G. Skinner, S.H. Wemple, J. Appl. Phys. 37 (1966) 388.
[12] S. Triebwasser, Phys. Rev. 114 (1959) 63.
[13] X.P. Wang, J.Y. Wang, H.J. Zhang, Y.G. Yu, W.L. Gao, R.I. Boughton, J. Appl. Phys. 103 (2008) 033513.
[14] W.D. Ma, Z.S. Zhao, S.M. Wang, D.M. Zhang, D.S. Xu, X.D. Wang, Z.J. Chen, Phys. Status Solidi (a) 176 (1999) 985.
[15] S.R. Sashital, S. Krishnakumar, S. Esener, Appl. Phys. Lett. 62 (1993) 2917.
[16] C.J. Lu, A.X. Kuang, J. Mater. Sci. 32 (1997) 4421.
[17] S. Yilmaz, T. Venkatesan, R. Gerhar-Multhaupt, Appl. Phys. Lett. 58 (1991) 2479.
[18] J. Bursik, V. Zelezny, P. Vanek, J. Eur. Ceram. Soc. 25 (2005) 2151.
[19] K. Suzuki, W. Sakamoto, T. Yogo, S. Hirano, J. Am. Ceram. Soc. 82 (1999) 1463.
[20] A. Rousseau, M. Guilloux-Viry, E. Dogheche, M. Bensalah, D. Remiens, J. Appl. Phys. 102 (2007) 093106.
[21] A. Rousseau, V. Laur, S. Deputier, V. Bouquet, M. Guilloux-Viry, G. Tanne, P. Laurent, F. Huret, A. Perrin, Thin Solid Films 516 (2008) 4882.
[22] A.X. Kuang, C.J. Lu, G.Y. Huang, S.M. Wang, J. Cryst. Growth 149 (1995) 80.
[23] A. Onoe, A. Yoshida, K. Chikuma, Appl. Phys. Lett. 78 (2001) 49.
[24] B.M. Nichols, B.H. Hoerman, J.H. Hwang, T.O. Mason, B.W. Wessels, J. Mater. Res. 18 (2003) 106.
[25] X.L. Tong, K. Lin, D.J. Lv, M.H. Yang, Z.X. Liu, D.S. Zhang, Appl. Surf. Sci. 255 (2009) 7995.
[26] W.L. Yang, Z.X. Zhou, B. Yang, Y.Y. Jiang, H. Tian, D.W. Gong, H.G. Sun, W. Chen, Appl. Surf. Sci. 257 (2011) 7221.
[27] W.L. Yang, Z.X. Zhou, B. Yang, R. Zhang, Z. Wang, H.Z. Chen, Y.Y. Jiang, J. Am. Ceram. Soc. 94 (2011) 2493.
[28] C.R. Cho, A. Grishin, Appl. Phys. Lett. 75 (1999) 268.
[29] X.Z. Liu, S.M. He, D.H. Li, Q.F. Lu, Z.H. Wang, S.X. Bao, Y.R. Li, J. Mater. Sci. 40 (2005) 5139.
[30] A. Liu, J. Xue, X. Meng, J. Sun, Z. Huang, J. Chu, Appl. Surf. Sci. 254 (2008) 5660.
[31] S. Loheide, S. Riehemann, F. Mersch, R. Pankrath, E. Kratzig, Phys. Status Solidi (a) 137 (1993) 257.